ELSEVIER

Journal of Biomechanics 40 (2007) 2244–2253

JOURNAL OF BIOMECHANICS

www.elsevier.com/locate/jbiomech
www.JBiomech.com

Random-walk models of cell dispersal included in mechanobiological simulations of tissue differentiation

M.A. Pérez[a,b], P.J. Prendergast[a,*]

[a]Trinity Centre for Bioengineering,School of Engineering, Trinity College, Dublin, Ireland
[b]Group of Structural Mechanics and Material Modelling, Aragón Institute of Engineering Research (I3A), University of Zaragoza, Zaragoza, Spain

Accepted 18 October 2006

Abstract

Computational models have shown that biophysical stimuli can be correlated with observed patterns of tissue differentiation, and simulations have been performed that predict the time course of tissue differentiation in, for example, long bone fracture healing. Some simulations have used a diffusion model to simulate the migration and proliferation of cells with the differentiating tissue. However, despite the convenience of the diffusion model, diffusion is not the mechanism of cell dispersal: cells disperse by crawling or proliferation, or are transported in a moving fluid. In this paper, a random-walk model (i.e., a stochastic model), with and without a preferred direction, is studied as an approach to simulate cell proliferation/migration in differentiating tissues and it is compared with the diffusion model. A simulation of tissue differentiation of gap tissue in a two-dimensional model of a bone/implant interface was performed to demonstrate the differences between diffusion vs. random walk with a preferred direction. Results of diffusion and random-walk models are similar with respect to the change in the stiffness of the gap tissue but rather different results are obtained regarding tissue patterning in the differentiating tissues; the diffusion approach predicted continuous patterns of tissue differentiation whereas the random-walk model showed a more discontinuous pattern—histological results are not available that can unequivocally establish which is most similar to experimental observation. Comparing isotropic to anisotropic random walk (preferred direction of proliferation and cell migration), a more rapid reduction of the relative displacement between implant and bone is predicted. In conclusion, we have shown how random-walk models of cell dispersal and proliferation can be implemented, and shown where differences between them exist. Further study of the random-walk model is warranted, given the importance of cell seeding and cell dispersal/proliferation in many mechanobiological problems.

Keywords: Mechanobiology; Mesenchymal stem cells (MSCs); Migration; Proliferation; Tissue differentiation; Random walk; Anisotropic

1. Introduction

According to van der Meulen and Huiskes (2002), skeletal mechanobiology aims to discover how mechanical forces modulate morphological and structural fitness of the skeletal tissues—bone, cartilage, ligament, and tendon. The first theoretical models in this field may be attributed to Pauwels (1941), who showed that the likely patterns of cell deformation in the fracture callus correlate with histological observations of tissue phenotype (Carter and Beaupré, 2001). Mechanobiological models have been used to explain mechanoregulation in fracture healing (Carter et al., 1988; Claes and Heigele, 1999; Lacroix and Prendergast, 2002; García et al., 2002; Doblaré et al., 2004; Isaksson et al., 2006), callus growth (Gómez-Benito et al., 2005), distraction osteogenesis (Morgan et al., 2006), osteochondral defect healing (Duda et al., 2005; Kelly and Prendergast, 2005), bone ingrowth into porous-coated implants (Simmons and Pilliar, 2000; Andreykiv et al., 2005), and tissue engineering (Kelly and Prendergast, 2006). Geris et al. (2004) have been able to use these models to predict the general patterns of tissue differentiation in bone ingrowth chambers attached to rabbit tibia. The proliferation/migration of cells has been modelled in previous studies by considering it to be analogous to

*Corresponding author. Tel.: +353 1 608 3393; fax: +353 1 679 5554.
E-mail address: pprender@tcd.ie (P.J. Prendergast).

0021-9290/$ - see front matter © 2006 Elsevier Ltd. All rights reserved.
doi:10.1016/j.jbiomech.2006.10.020

diffusion (Lacroix et al., 2002). Bailon-Plaza and van der Meulen (2003) modelled cell migration as a diffusive process taking into account gradients in matrix density (haptotaxis). However, using a diffusion model to simulate cell dispersal means that proliferation and migration tend to create a smooth variation in cell density, but such a constraint is not physiological nor is it necessary if a more general random-walk model is used. Furthermore, random-walk models can simulate not only a preferred direction to migration (resulting from, for e.g., convection or chemoattractant control of migration) but proliferation can also be explicitly modelled by multiplying cell numbers during dispersal. Moreover, using a random-walk model these aspects could be included for several cell populations simultaneously.

Experiments demonstrating random movement of cells were done many years ago. For example, Ambrose (1961) observed the movement of an isolated fibroblast over the surface of a tissue culture dish as mostly random while Carter (1965) was among the first to demonstrate that cells execute a random walk on surfaces. Gail and Boone (1970) quantified that cell migration differs from the pure random walk in that the angles between successive turns are closer to zero; therefore, cells show persistence in their movements. More recently, Palsson and Bhatia (2004) observed, in an in vivo analysis, that a random spatial distribution could be produced during stem cell proliferation. Zohar et al. (1998) observed experimentally that mesenchymal stem cells (MSCs) disperse by crawling and convection in the fluid. The directional nature of movement is most apparent with fibroblasts; during wound healing, they become highly motile and migrate in large numbers towards the wound (Spyrou et al., 1998); diffusion-type models that reproduce this effect have been developed (Tranquillo and Murray, 1992; Dale et al., 1997). Therefore, both the random and the directional nature of cell movement have been described but neither have been investigated or compared with the diffusion model for mechanobiology simulations.

In pursuit of a better understanding of the role of the proliferation and migration of cells on tissue regeneration, we combined the mechanoregulation algorithm for tissue differentiation proposed by Prendergast et al. (1997) with a random-walk approach for cell proliferation and migration. We hypothesise that the random-walk approach to simulating cell dispersal in mechanobiological simulations will give different patterns of tissue differentiation compared to the diffusion model, and furthermore that the inclusion of *a preferred direction* will also make a difference for the results of the simulation. We test these hypotheses in a finite element (FE) model of osseointegration at a bone/implant gap. If these hypotheses are corroborated, it would suggest that mechanobiological simulations can be improved using random-walk models of cell dispersal in the regenerating tissue.

2. Methods

2.1. Cell proliferation

Two approaches for modelling the proliferation of cells based on the random-walk theory are developed: an isotropic one and an anisotropic one—in the latter cell migration and proliferation have a preferred direction. In both cases, it is a stochastic process. Initially, a cell is presumed (in two dimensions) to be surrounded by four locations that a daughter cell could occupy (Fig. 1). Daughter cells are also allowed to remain in the position of the parent cell but opposite "poles" are excluded (as shown in Fig. 1) because adjacent positions are far more likely to occur during mitosis. When *isotropic* mitosis is assumed, then cells can occupy neighbouring positions with equal probability p (see Fig. 1). Although Fig. 1 shows four free positions around the cell, this will not, in general, be the case because some positions may already be occupied. Therefore the model incorporates "contact inhibition" by checking for vacant positions while cells proliferate and depending on the available states (n), the value of the probability p is computed in order to fulfil the condition $\sum_{i=1}^{n} p_i = 1$. If all the surrounded positions are free, the probability p given in Fig. 1 will be equal to $\frac{1}{8}$. If there is only one vacant position, the probability that it will be filled is equal to one. If all neighbouring positions are occupied, mitosis will not occur.

More generally, cells may disperse with a preferential direction of proliferation—this implies *anisotropic* proliferation. The possible states that a cell can occupy after mitosis, if there is a preferred direction with its corresponding probability, are illustrated in Fig. 2. The highest probability positions are the ones in which one daughter cell tends to appear in a preferred direction (in this case, downwards) with p_1 probability (three first states in Fig. 2 or generally n_1 possible states), while the others positions were computed with probability of p_2 (n_2 possible states) or p_3

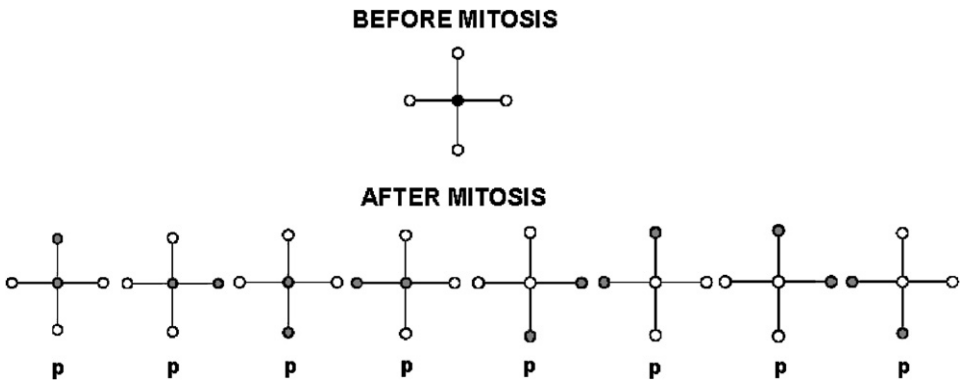

Fig. 1. Possible states that daughter cells can occupy after mitosis. The distance between sites is only schematic; adjacent sites in the algorithm are considered to be exactly the diameter of an MSC (Lanza et al., 2005).

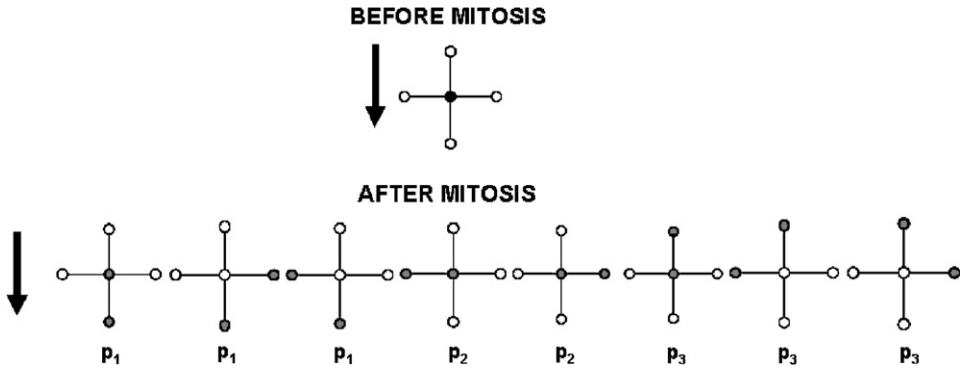

Fig. 2. Possible states that daughter cells can occupy after mitosis with anisotropic proliferation direction (preferred direction is given by the arrow).

(n_3 possible states) depending on the position of one of the daughter cells (Fig. 2). In *anisotropic* proliferation, the neighbouring cell positions are also checked and, depending on the available states, the corresponding value of p is computed fulfilling $\sum_{i=1}^{n_1} p_1 + \sum_{i=1}^{n_2} p_2 + \sum_{i=1}^{n_3} p_3 = 1$. In this study, a strong preferred direction was assumed as $p_1 = 10p_2 = 60p_3 = p$; in this case, p can be calculated to be $\frac{4}{13}$. Probability values are empirical and would need to be measured by experiment.

2.2. Cell migration

Cell migration was also based on the stochastic random-walk approach. Recognising that migration is a more rapid process, a new location for a migrating cell is chosen several times during one iteration of the proliferation process. In the simulations presented here, five random jumps are performed for each cell for each iteration of the simulation. At the end of the migration if that position is free is checked. In the event that the location has already been occupied by another cell, a neighbouring location is chosen again randomly, except if the cell population is large enough to prevent the migration of cells. In that case, cells remain in their initial position without migrating.

2.3. Mechanoregulation model

Following Prendergast et al. (1997), two biophysical stimuli (octahedral shear strain γ and relative fluid/solid velocity v) are used to regulate tissue differentiation. The octahedral shear strain is computed by means of the principal strains (ε_{I}, $\varepsilon_{\mathrm{II}}$, $\varepsilon_{\mathrm{III}}$) as $\gamma = 1/3\sqrt{(\varepsilon_{\mathrm{I}} - \varepsilon_{\mathrm{II}})^2 + (\varepsilon_{\mathrm{I}} - \varepsilon_{\mathrm{III}})^2 + (\varepsilon_{\mathrm{II}} - \varepsilon_{\mathrm{III}})^2}$. This theory proposed that the mechanical environment in the tissue has a controlling influence on tissue differentiation according to a stimulus S where $S = \gamma/a + v/b$, where $a = 0.0375$; $b = 3\,\mu\mathrm{m/s}$; these constants were derived by Huiskes et al. (1997). High levels of stimuli ($\gamma/a + v/b > 3$) promotes the differentiation of MSCs into fibroblasts, intermediate levels ($\gamma/a + v/b > 1$ and $\gamma/a + v/b < 3$) stimulate the differentiation into chondrocytes and low levels ($\gamma/a + v/b < 1$) favour the differentiation of osteoblasts from the MSC pool. Cells then synthesise the appropriate extracellular matrix leading to tissue formation and new mechanical properties for the tissue.

2.4. FE model

A two-dimensional FE model of a bone/implant interface was generated to simulate the bone ingrowth process, which included a bone and implant layer and the interfacial gap of regenerating tissue. The implant surface was 10 mm long and the bone/implant gap was of 1.0 mm (Fig. 3). The model consists of 3000 4-noded elements. The bone and the interfacial gap used poroelastic 4-noded quadrilateral elements. The cell proliferation/migration approach is performed in a lattice inside each FE in the interfacial gap tissue (Fig. 3). The distance between lattice points is 0.01 mm giving 100 lattice points inside each FE. Therefore, the cell diameter is assumed to be equal for each cell type, 10 μm giving 10,000 cells/mm^2 (Lanza et al., 2005).

Initially, the interfacial gap was assumed to be filled with granulation tissue. The bone surrounding the gap was included with properties of cortical bone and the implant was modelled as homogenous, isotropic and linear elastic with an elastic modulus of 100 GPa and a Poisson's ratio of 0.3. The material properties used for each tissue type are listed in Table 1.

Restraints were placed along the bone surface as shown in Fig. 3 with the pore fluid pressure set to zero. Two types of loads were applied: shear forces or prescribed displacements. The magnitude of the shear force was computed to obtain an initial relative displacement between the bone and implant surface of either 150 or 500 μm. This shear force is applied throughout the simulation; note that the displacement reduces as the tissue stiffens. On the other hand, a prescribed displacement produces a situation were a relative displacement between bone and implant of either 150 or 500 μm is maintained throughout the simulation (displacement-control) and the force generated at peak displacement increases.

2.5. Implementation of the mechanobiological model

MSCs invade the bone/implant interface through the bone surface in both the diffusion and random-walk approaches. In addition, a small percentage of the maximum concentration of cells is allowed within the interfacial gap (1%) assuming to be randomly distributed from the very beginning of the simulation as MSCs. Once some minimum time (*cell age*) has elapsed for a cell (in this simulation the minimum time is set at seven iterations), MSCs may differentiate into fibroblasts, chondrocytes, or osteoblasts depending on the mechanical stimulus, producing different tissue types (fibrous tissue, cartilage, or bone, respectively). The shear strain and fluid/solid velocity needed were computed from a poroelastic analysis performed using Abaqus v.6.5 (Hibbit, Karlsson and Sorensen, Inc., 2005).

The rate cell movement during proliferation and migration is different for each type of cell and corresponds to the diffusion coefficients shown in Table 1. Diffusion coefficients for each cell type are calculated as the weighted average of the diffusion coefficients for each of the tissue types at that site in the model (Kelly and Prendergast, 2005).The number of MSCs that differentiate in each iteration i in each element of the FE model is computed multiplying the *differentiation rate* (assumed as 0.3) by the number of MSCs that have reached the critical age ($i > 7$) at that element. When MSCs differentiate a new tissue type is predicted so the material properties in the element change. It could happen that in some elements granulation tissue and only one differentiated tissue type (cartilage, bone, or fibrous tissue) exist simultaneously; the new material properties (modulus of elasticity and permeability) are calculated based on the concentration of differentiated cells c_t (three cell/tissue types) with respect to the maximum concentration of cells allowed in each element $c_{\max}$. For example, the Young's modulus of each element would be calculated as

$$E = \frac{c_t}{c_{\max}} E_{\text{differentiated}} + \frac{c_{\max} - c_t}{c_{\max}} E_{\text{granulation}},$$

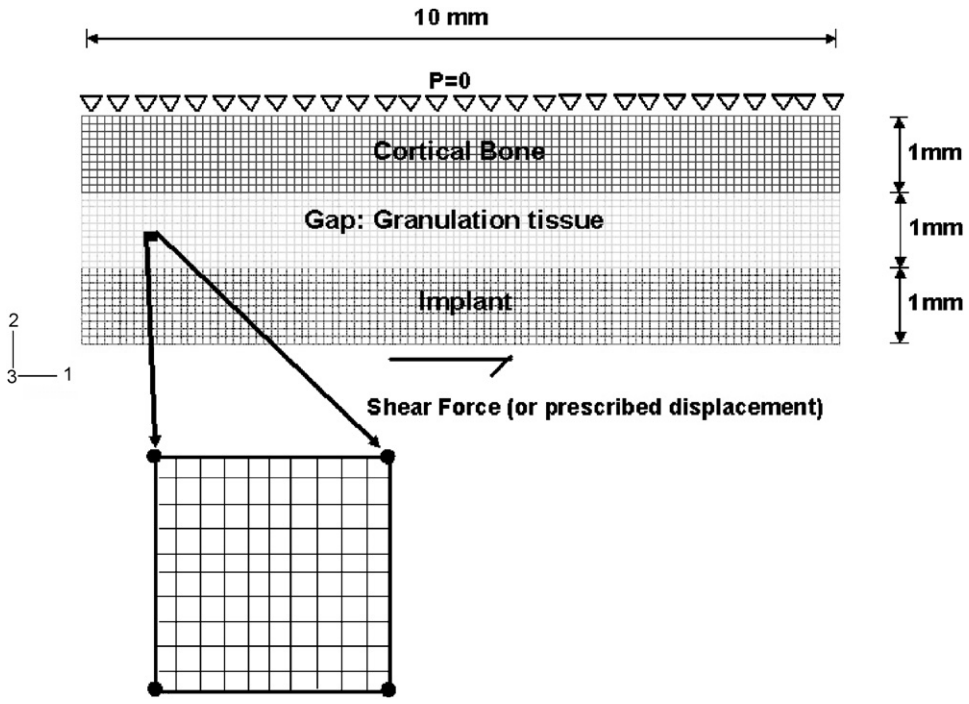

Fig. 3. FE model of the bone ingrowth simulation and the lattice where the cell proliferation/migration is performed.

Table 1
Material properties

	Granulation tissue	Fibrous tissue	Cartilage	Immature bone	Cortical bone
Young's modulus (MPa)	0.2	2[a]	10[a]	1000	17000.0[c]
Permeability ($m^4/N\,s \times 10^{-14}$)	1	1[a]	0.5[a]	0.1	0.001[b]
Poisson's ratio	0.167	0.167	0.3	0.3	0.3
Bulk solid modulus (MPa)	2300[d]	2300[d]	3700[d]	13940[d]	13920.0[d]
Diffusion coefficient (mm^2/iteration)	0.8	0.1	0.05	0.01	

[a]Hori and Lewis (1982).
[b]Cowin (1999).
[c]Kelly and Prendergast (2005).
[d]Lacroix and Prendergast (2002).

where $E_{\text{differentiated}}$ is the Young's modulus of the corresponding type of tissue (fibrous, cartilage, or bone). Instantaneous changes of tissue type in an element is prevented computing the average material properties from the ten previous iterations.

When the stimulus on an element containing both granulation tissue and a differentiated tissue changes such that the differentiated cell type is under an inappropriate mechanical stimulus, the differentiated cells are removed by apoptosis; therefore, only one differentiated cell type occurs in each element. No de-differentiation or trans-differentiation is considered, although it would straightforward to include this in the model if necessary. Each of these cellular events was implemented into an algorithm (Fig. 4).

2.6. Implementation of a diffusion model

The diffusion model of cell proliferation and migration uses

$$\frac{dc_t}{dt} = D_t \nabla^2 c_t + p(c_t)c_t, \quad (1)$$

where c_t is the cell concentration within the interfacial gap. The first term on the right-hand side of Eq. (1) describes cell migration by linear diffusion, where D_t is the diffusion coefficient (see Table 1) and the second term describes the proliferation rate per cell. In the random-walk model, the proliferation rate decreases as the contact inhibition increases, i.e., as c_t increases. To allow for comparison between the two models a proliferation rate was calculated as $p(c_t) = Ae^{-bc_t}$, where A and b were computed to be 1.8237 and 6×10^{-6}.

3. Results

3.1. Isotropic random-walk vs. diffusion analysis under force-control

Under force-control (i.e., with a cyclic shear force computed to give an initial micromovement of 500 μm), the relative displacement between bone and implant decreased over time with both the isotropic random walk and the diffusion approach (Fig. 5). Different fractions of

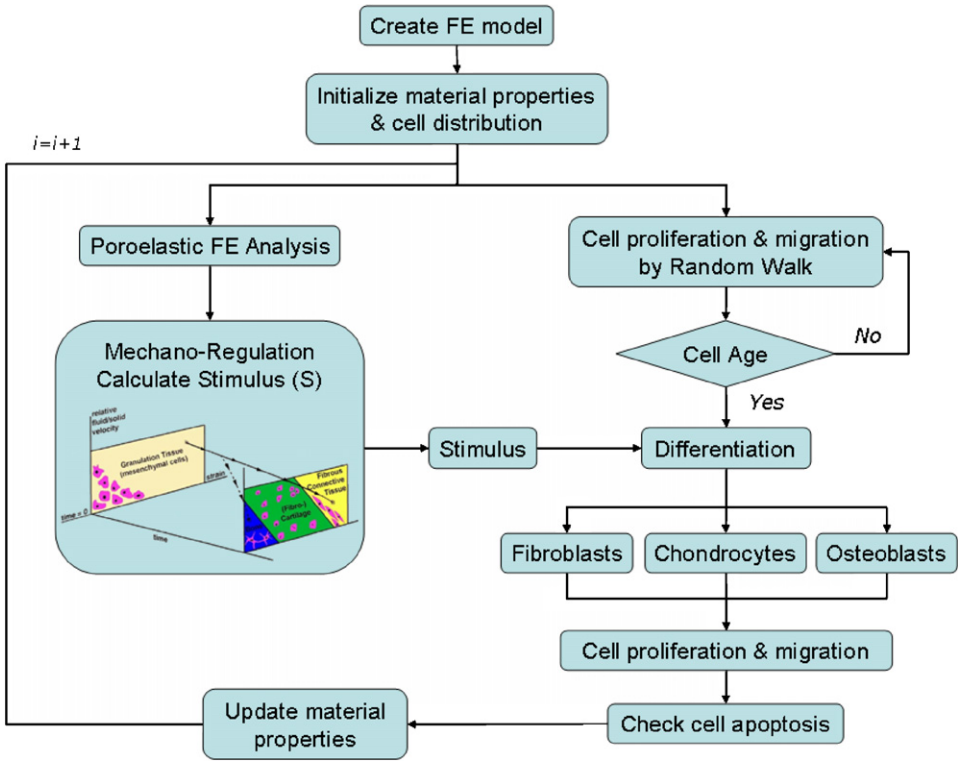

Fig. 4. Flow chart diagram of computational algorithm to model the mechanobiological model which combines the results of a poroelastic analysis with the new isotropic/anisotropic approach for cell migration and proliferation.

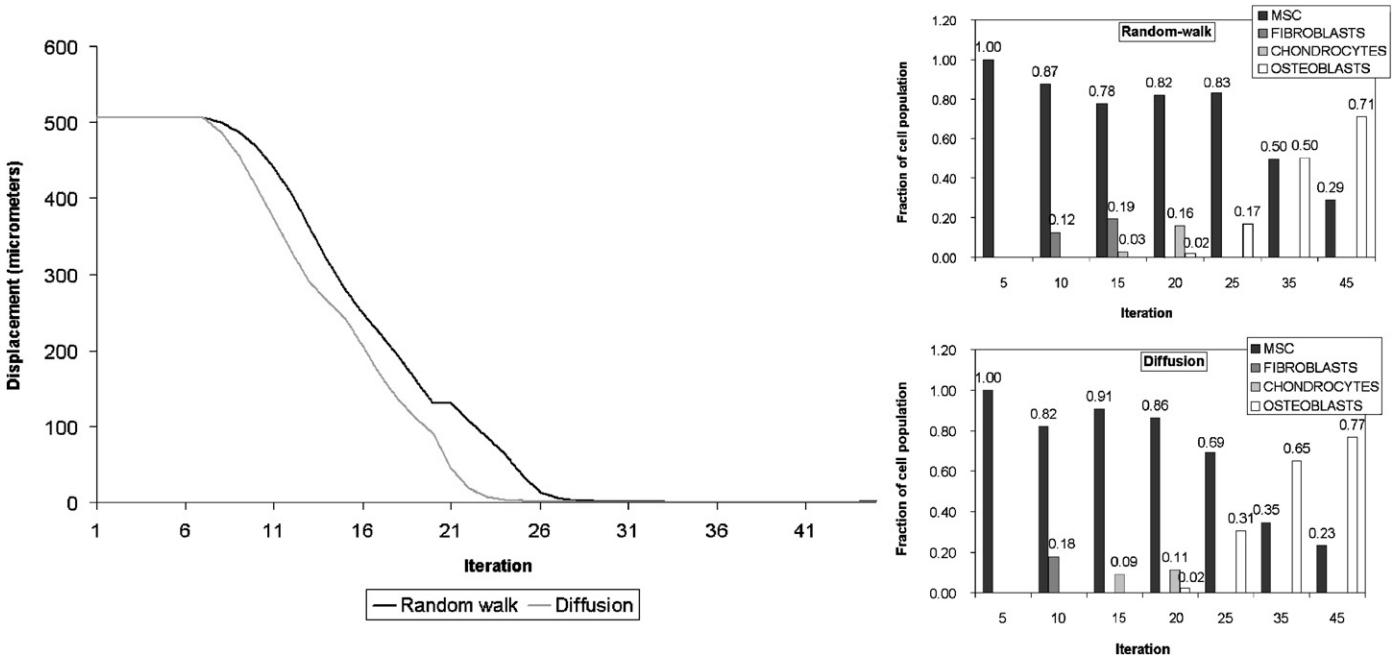

Fig. 5. Micromotion and fraction of the different cell types predicted at the bone/implant interface, with isotropic cell movement and force-control under shear loading to obtain an initial relative displacement of 500 μm comparing the random walk with a diffusion model.

cell types were also predicted at the bone/implant interface (Fig. 5).

Different tissue differentiation patterns were computed for random walk compared to diffusion (Fig. 6); the diffusion analysis predicted a continuous distribution of tissues (Fig. 6(a)), whereas the random-walk model (isotropic cell proliferation—Fig. 6(b)) predicted a clearly non-homogeneous cell and tissue distribution. In fact, islands of MSCs, fibroblasts, chondrocytes, and osteoblasts appear instead of a smoothly varying distribution of the

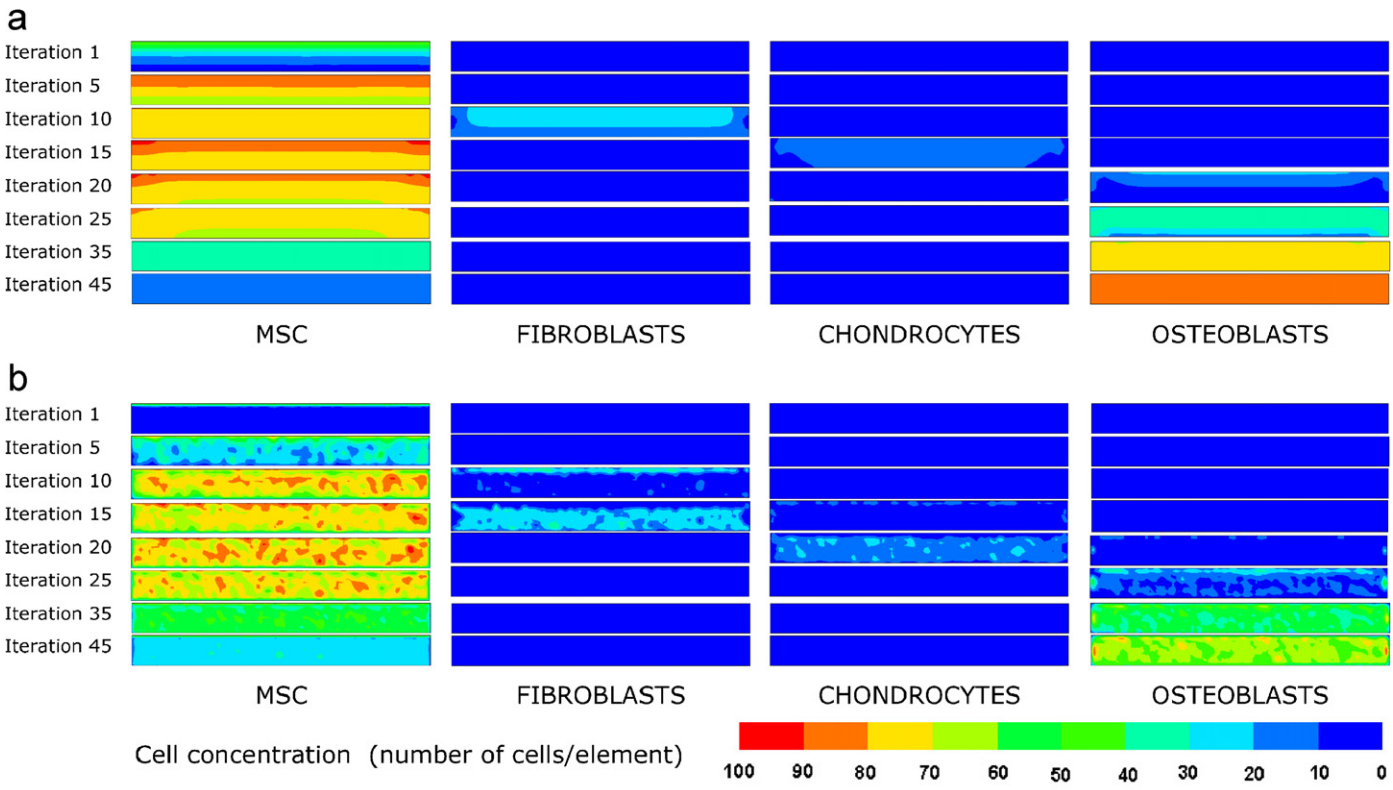

Fig. 6. Predicted cell distribution at the bone/implant interface under shear force-control analysis to obtain an initial displacement of 500 μm with (a) diffusion analysis and (b) isotropic cell proliferation (random-walk model).

different cell types. Initially, there are MSCs at the bone surface and randomly distributed in the bone/implant interfacial gap (iteration 1) that proliferate as the simulation continues (iteration 5). As MSCs differentiate, new tissue with new material properties appears, so the stimulus changes predicting fibroblast apoptosis. Then the new and remaining MSCs differentiate into cartilage and bone depending on the value of the stimulus (iterations 10, 15, till iteration 35). In the last iteration the number of osteoblasts is considerably high in both analyses (Fig. 6); the consequence is a low degree of micromovement reduction at the bone/implant interface (Fig. 5).

The random-walk approach proposed in this paper is based on a stochastic methodology; therefore in order to verify how repetitive the simulation outcome was, five force-control simulations were performed and the results compared. The relative displacements predicted were very similar, but not identical (data not shown).

3.2. Isotropic vs. anisotropic random walk under force-control

Isotropic vs. anisotropic random-walk models show small but consistent differences—anisotropic cell proliferation/migration model reduces the displacements more rapidly (Fig. 7). Furthermore, at the end of the simulation assuming the random-walk model with the anisotropic approach, the fraction of osteoblasts is slightly higher than with the isotropic model (0.76 compared to 0.71).

3.3. Change in mechanical stimuli

Octahedral shear strain and fluid/solid velocity changed in the gap tissue during differentiation. As an example, take anisotropic proliferation under shear force-control: octahedral shear strain reduces monotonically whereas fluid/solid velocity evolution is rather complicated (Fig. 8). At the early stage of the simulation, the fluid flow is very small in the three positions considered. But as the simulation continues, and the fibrous tissue and cartilage formed, it starts to increase. Also, fluid/solid velocity was predicted to increase when bone began to differentiate.

3.4. Displacement-control vs. force-control

A comparison between force-control and displacement-control was also performed. During motion-control, the micromotion of 150 or 500 μm is maintained during tissue formation. The initial force to produce a micromotion of 150 μm is lower than for 500 μm, but as the tissue differentiation occurs a higher force is needed to produce a lower relative displacement between the bone and implant (Fig. 9). This result is explained by considering that tissue differentiates to form bone under 150 μm

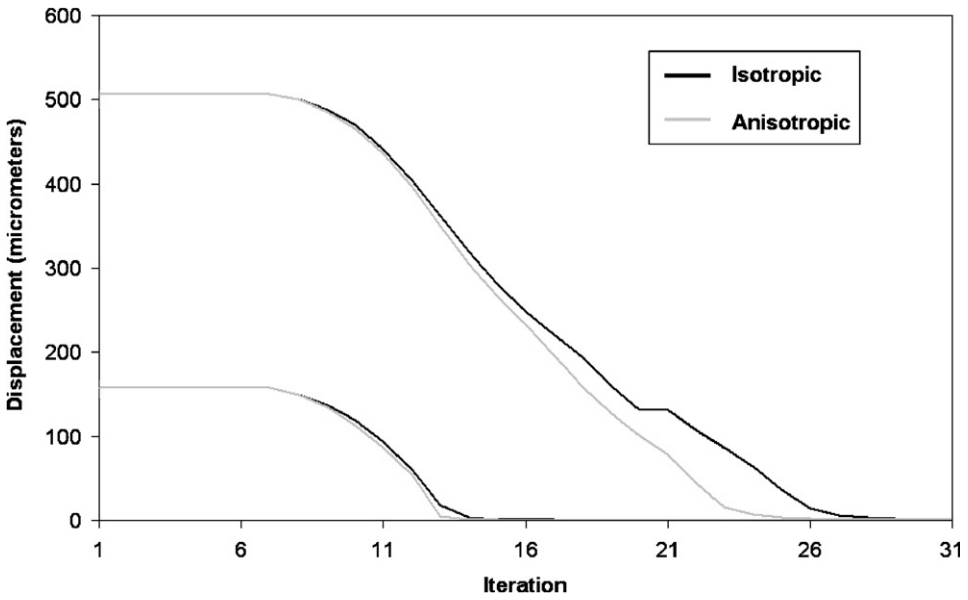

Fig. 7. Micromotion predicted at the bone/implant interface with isotropic and anisotropic cell movement and force-control to obtain initial relative displacement (150 or 500 μm).

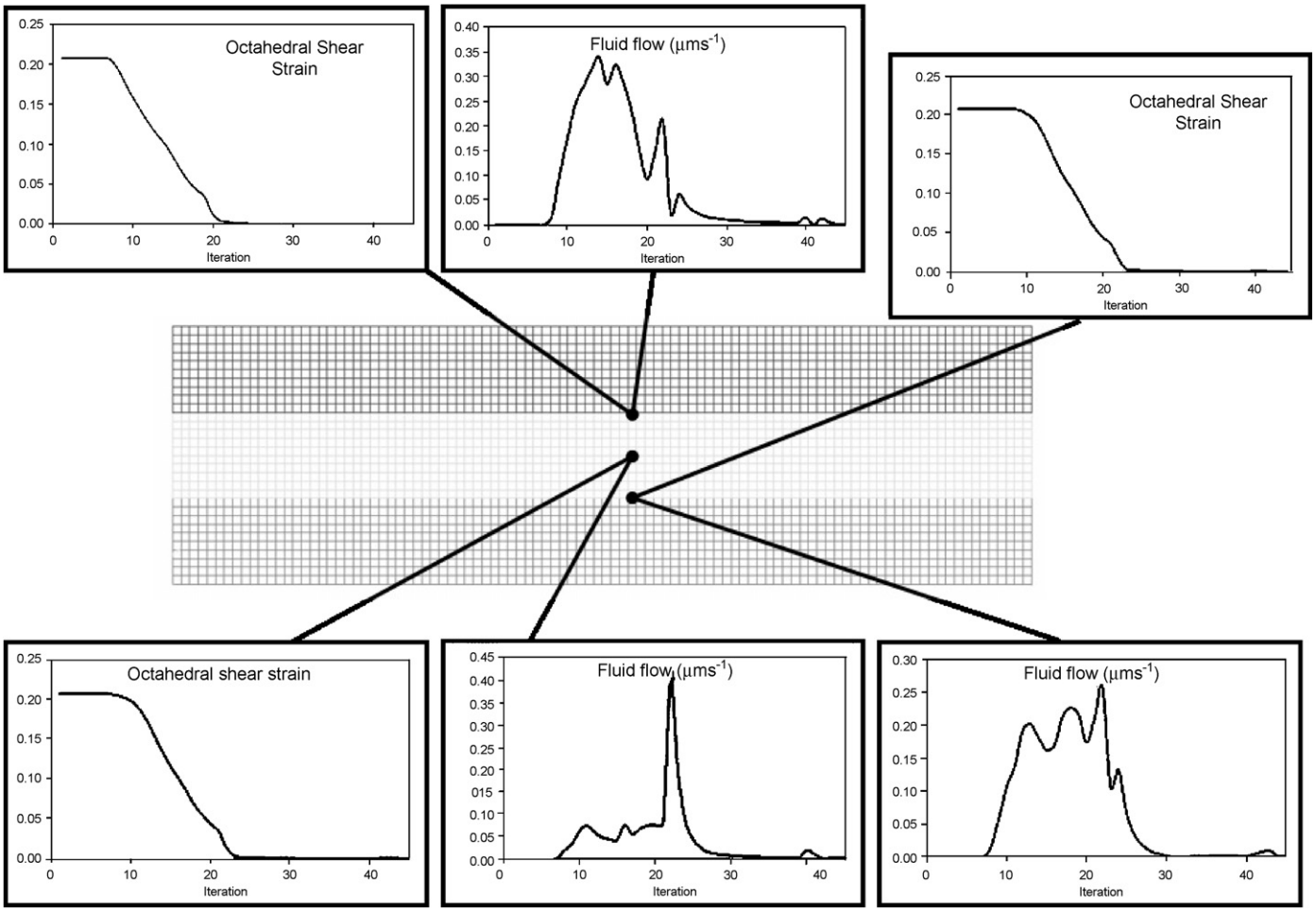

Fig. 8. Prediction of octahedral shear strain and fluid/solid velocity at the bone/implant interface with anisotropic proliferation under shear force-control analysis to obtain an initial displacement of 500 μm.

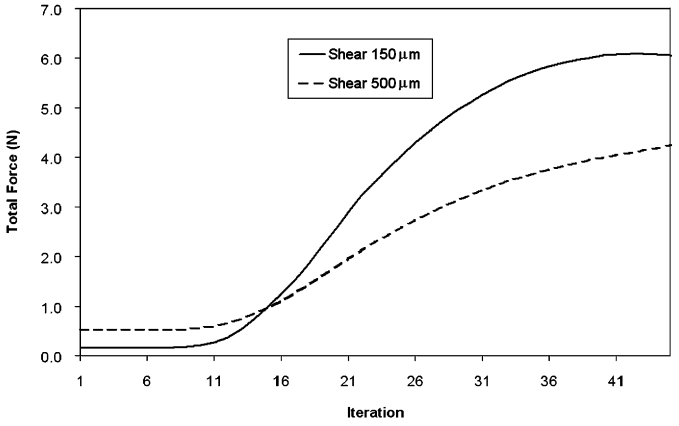

Fig. 9. Force predicted at the bone/implant interface with anisotropic cell movement under displacement-control for two different relative displacements.

displacement thus requiring a large force to keep that displacement constant (Fig. 10(a)), whereas under a displacement-control of 500 μm, bone formation does not ensue so the force required to maintain the 500 μm displacement remains low (Fig. 10(b)). Thus it is important to distinguish force-control and displacement-control in tissue differentiation simulations.

4. Discussion

The computational model presented here is an attempt to further develop computational schemes for modelling tissue differentiation by exploring the use of the random-walk approach as a methodology for modelling the proliferation/migration behaviour of cell populations. We have shown how the random-walk model can be implemented and shown that, regarding force/displacement behaviour it gives similar results to the diffusion approach but as regards tissue differentiation patterns it can give different results. However the random walk does have methodological advantages, viz. the easy implementation of anisotropic migration/proliferation, cell seeding, and the constraints on proliferation. Nonetheless, the approach implemented here still suffers from many simplifications; for instance, it is assumed that all cell phenotypes (fibroblasts, chondrocytes, and osteocytes) proliferate at the same rate as MSCs. In reality, these types of cells proliferate at a lesser extent than MSCs. Another limitation is that the differentiation rate assumed is a phenomenological one—no experimental values have been found. The minimum time for MSC differentiation (*cell age*) was assumed equal for all cell types whereas this value probably differs from one cell type to another. Another assumption is the number of cell migration steps, or 'jumps' per iteration; however, considering more than five jumps does not influence the final result of the simulations (data not shown). Regarding the mechanoregulation diagram for tissue differentiation, the boundaries have yet to be established experimentally, although their values are consistent with previous studies (Huiskes et al., 1997; Lacroix and Prendergast, 2002; Geris et al., 2004; Andreykiv et al., 2005; Kelly and Prendergast, 2005; Isaksson et al., 2006; Kelly and Prendergast, 2006). The FE model used to simulate the interfacial gap between bone and implant is also a simplification compared to the real complex geometry found for real dental or orthopaedic implants; in reality the surface topography presents many irregularities that can only be analysed with a three-dimensional (3D) FE model; an implementation of the algorithms in 3D is under development (Byrne et al., 2006).

Turning to the differences between the diffusion approach and the random-walk approach, the reduction in implant/bone micromovements predicted with both approaches are quite similar and make the same prediction, i.e., excessive bone/implant micromovements inhibit bone ingrowth and lead to the development of a fibrous membrane. On the other hand, patterns of tissue differentiation predicted by means of the random-walk approach (both isotropic cell proliferation and anisotropic cell proliferation/migration) are somewhat different than the results obtained by diffusion models. A continuous and relatively smooth change cell distribution (MSCs, fibroblasts, chondrocytes, or osteoblasts inside the interfacial gap) is predicted with a diffusion analysis (Fig. 6(a)), whereas the random-walk model predicts a more irregular distribution (Fig. 6(b)) with local peaks of cell concentration. The results with the random walk do show some similarity with histological observations of osseointegration in that clusters of cells appear (see, for example, Bechtold et al., 2001; Götz et al., 2004); however, the similarity is not sufficient to be considered a corroboration of the random-walk approach and, in any case, not only could random movement of cells contribute to heterogeneous tissue distribution, but also other factors not considered in this study such as gradients in biochemical factors, nutrients, oxygen, or vascularity could also be important. Finally, consideration should be given to the appropriate length scale in mechanobiological simulations.

Prendergast et al. (1997) present the change in biophysical stimuli during mechanoregulated tissue differentiation as a curve in R^3 (two biophysical stimuli and time). If the situation is such that a certain motion is maintained (displacement-control) then the shear strain stays high and no bone will form, instead soft tissue will be maintained (Fig. 10), whereas if the synthesis of extracellular matrix permits a reduction in motion (force-control) then the shear strains and fluid velocities will reduce and a mechanical milleau allowing ossification will be achieved through intermediate tissue types (fibrous and cartilage tissue). Therefore, the use of random-walk models to simulate cell migration and proliferation agree with other computational studies on the importance of differentiating force-control from displacement-control environments (Prendergast, 2004).

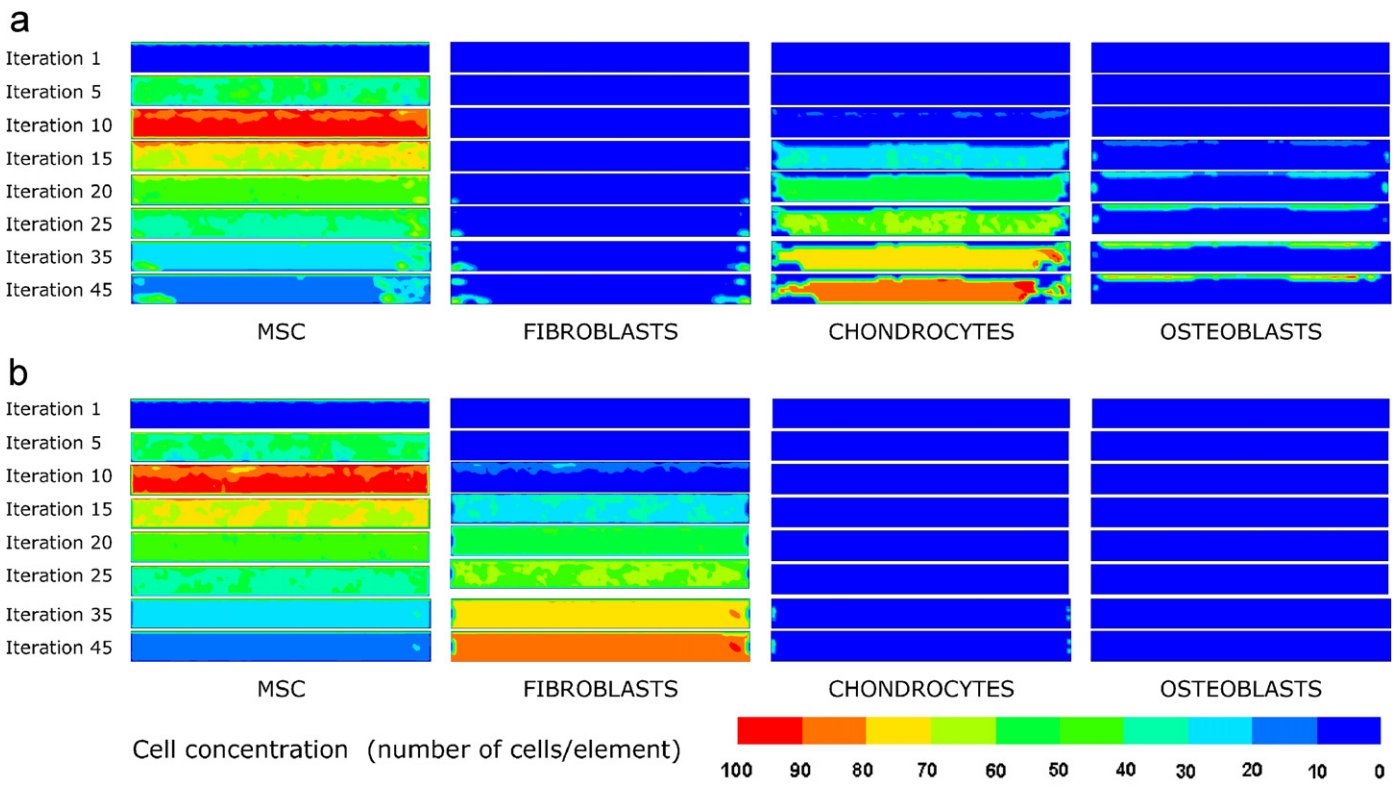

Fig. 10. Predicted cell distribution at the bone/implant interface with anisotropic cell movement under displacement-control for a relative displacement of (a) 150 μm and (b) 500 μm.

One example of an application of the anisotropic random-walk model is the prediction of osseointegration in HA-coated vs. uncoated orthopaedic implants because the former are assumed to enhance osteoconductivity and to provide a more favourable environment for tissue differentiation (Kieswetter et al., 1996). Although the mechanisms by which calcium phosphate coatings promote osteoconduction are not yet clear, both implant topography and surface chemistry are believed to be important (Buser et al., 1991) and surface topography may have an effect on osteoprogenitor cell migration (Davies, 1998).

In conclusion, random-walk stochastic models presented in this paper provide a mechanistic approach to simulating cell behaviour during differentiation particularly as regards proliferation and movement modelling—in this respect it is, we suggest, a more powerful methodology for mechanoregulation algorithms for tissue differentiation, and could be improved in the future by including other important cellular events relevant to problems in tissue engineering such as cell trans-differentiation and the development of vascular channels in the form of preferred movement paths for oxygen/nutrients. Our predictions also show that the random-walk model of cell dispersal during tissue differentiation gives heterogeneous tissue distribution whereas the diffusion model does not; we have not been able to show conclusively which best matches histological observation, such an analysis awaits further study.

Acknowledgments

This work was performed when the first named author was on sabbatical leave from the University of Zaragoza to Trinity College Dublin. Some sponsorship was provided by the PRTLI Cycle 3, administered by the HEA in Ireland and the Cai-Europe Program for Research Staying. It is a pleasure to thank Dr. Manuel Doblaré and Dr. José Manuel García-Aznar for making possible this sabbatical period and their continued support during these months.

References

Ambrose, E.J., 1961. The movements of fibrocytes. Experimental Cell Research 8, 54–73.

Andreykiv, A., Prendergast, P.J., van Keulen, F., Swieszkowski, W., Rozing, P.M., 2005. Bone ingrowth simulation for a concept glenoid component design. Journal of Biomechanics 38 (5), 1023–1033.

Bailon-Plaza, A., van der Meulen, M.C.H., 2003. Beneficial effects of moderate, early loading and adverse effects of delayed or excessive loading on bone healing. Journal of Biomechanics 36, 1069–1077.

Bechtold, J.E., Kubic, V., Søballe, K., 2001. A controlled experimental model of revision implants. Part I. Development. Acta Orthopaedica Scandinavica 72 (6), 642–649.

Buser, D., Schenk, R.K., Steinemann, S., Fiorellini, J.P., Fox, C.H., Stich, H., 1991. Influence of surface characteristics on bone integration of titanium implants. A histomorphometric study in miniature pigs. Journal of Biomedical Materials Research 25, 889–902.

Byrne, D.P., Kelly, D.J., Prendergast, P.J., 2006. Optimisation of scaffold porosity using a stochastic model for cell proliferation and migration

in mechanobiological simulations. Journal of Biomechanics 39 (suppl. 1), 5413–5414.
Carter, S.B., 1965. Principles of cell motility: the direction of cell movement and cancer invasion. Nature 208 (16), 1183–1187.
Carter, D.R., Beaupré, G.S., 2001. Skeletal function and form. Mechanobiology of skeletal development, aging, and regeneration. Cambridge University Press, Cambridge.
Carter, D.R., Blenman, P.R., Beaupré, G.S., 1988. Correlations between mechanical stress history and tissue differentiation in initial fracture healing. Journal of Orthopaedic Research 7, 398–407.
Claes, L.E., Heigele, C.A., 1999. Magnitudes of local stress and strain along bony surfaces predict the course and type of fracture healing. Journal of Biomechanics 32, 255–266.
Cowin, S.C., 1999. Bone poroelasticity. Journal of Biomechanics 32, 217–238.
Dale, P.D., Sherratt, J.A., Maini, P.K., 1997. Role of fibroblast migration in collagen fiber formation during fetal and adult dermal wound healing. Bulletin of Mathematical Biology 59 (6), 1077–1100.
Davies, J.E., 1998. Mechanisms of endosseous integration. International Journal of Prosthodontics 11, 391–402.
Doblaré, M., García, J.M., Gomez, M.J., 2004. Modelling bone tissue fracture and healing: a review. Engineering Fracture Mechanics 71, 1809–1840.
Duda, G.N., Maldonado, Z.M., Klein, P., Heller, M.O.W., Burns, J., Bail, H., 2005. On the influence of mechanical conditions in osteochondral defect healing. Journal of Biomechanics 38 (4), 843–851.
Gail, M.H., Boone, C.W., 1970. The locomotion of mouse fibroblasts in tissue culture. Biophysical Journal 10, 980.
García, J.M., Kuiper, J.H., Doblaré, M., Richardson, J.B., 2002. A numerical model to study the mechanical influences on bone fracture healing. In: Proceedings of the 13th Conference of European Society of Biomechanics, Wroclaw, Poland, pp. 394–395.
Geris, L., Andreykiv, A., van Oosterwyck, H., Vander Sloten, J., van Keulen, F., Duyck, J., Naert, I., 2004. Numerical simulation of tissue differentiation around loaded titanium implants in a bone chamber. Journal of Biomechanics 37, 763–769.
Gómez-Benito, M.J., García-Aznar, J.M., Kuiper, J.H., Doblaré, M., 2005. Influence of fracture gap size on the pattern of long bone healing: a computational study. Journal of Theoretical Biology 235, 105–119.
Götz, H.E., Müller, M., Emmel, A., Holzwarth, U., Erben, R.G., Stangl, R., 2004. Effect of surface finish on the osseointegration of laser-treated titanium alloy implants. Biomaterials 25, 4057–4064.
Hibbit, Karlsson and Sorensen, Inc., 2005. Abaqus User's Manual, v. 6.5. HKS Inc.
Hori, R.Y., Lewis, J.L., 1982. Mechanical properties of the fibrous tissue found at the bone-cement interface following total joint replacement. Journal of Biomedical Materials Research 16, 911–927.
Huiskes, R., van Driel, W.D., Prendergast, P.J., Søballe, K., 1997. A biomechanical regulatory model for periprosthetic fibrous-tissue differentiation. Journal of Materials Science: Materials in Medicine 8 (12), 785–788.
Isaksson, H., Wilson, W., van Donkellaar, C.C., Huiskes, R., Ito, K., 2006. Comparison of biophysical stimuli for mechano-regulation of tissue differentiation during fracture healing. Journal of Biomechanics 39 (8), 1507–1516.
Kelly, D.J., Prendergast, P.J., 2005. Mechano-regulation of stem cell differentiation and tissue regeneration in osteochondral defects. Journal of Biomechanics 38 (7), 1413–1422.
Kelly, D.J., Prendergast, P.J., 2006. Prediction of the optimal mechanical properties for a scaffold used in osteochondral defect repair. Tissue Engineering 12 (9), 2509–2519.
Kieswetter, K., Schwartz, Z., Hummert, T.W., Cochran, D.L., Simpson, J., Boyan, B.D., 1996. Surface roughness modulates the local production of growth factors and cytokines by ostoblast-like MG-63 cells. Journal of Biomedical Materials Research 32, 55–63.
Lacroix, D., Prendergast, P.J., 2002. A mechano-regulation model for tissue differentiation during fracture healing: analysis of gap size and loading. Journal of Biomechanics 35, 1163–1171.
Lacroix, D., Prendergast, P.J., Li, G., Marsh, D., 2002. Biomechanical model to simulate tissue differentiation and bone regeneration: application to fracture healing. Medical and Biological Engineering and Computing 40, 14–21.
Lanza, R., Thomas, E.D., Thomson, J., Pedersen, R., 2005. Essentials of Stem Cell Biology. Academic Press, New York.
Morgan, E.F., Longaker, M.T., carter, D.R., 2006. Relationships between tissue dilatation and differentiation in distraction osteogenesis. Matrix Biology 25 (2), 94–103.
Palsson, B.O., Bhatia, S.N., 2004. Tissue Engineering. Pearson Prentice Hall Bioengineering.
Pauwels, F., 1941. Grundiβ einer Biomechanik der Frakturheilun. In: 34th Kongress der Deutschen Orthopädischen Gesellschaft, Ferdinand Enke Verlag, Stuttgart, pp. 62–108.
Prendergast, P.J., 2004. Computational mechanobiology. In: Cerrolazza, M., Doblaré, M., Martínez, G., Calvo, B. (Eds.), Computational Bioengineering: Current Trends and Applications. Imperial College Press, pp. 117–133.
Prendergast, P.J., Huiskes, R., Søballe, K., 1997. Biophysical stimuli on cells during tissue differentiation at implants interfaces. Journal of Biomechanics 30 (6), 539–548.
Simmons, C.A., Pilliar, R.M., 2000. A biomechanical study of early tissue formation around bone-interfacing implants: the effect of implant surface geometry. EM Squared, Toronto, pp. 369–380.
Spyrou, G.E., Watt, D.A.L., Naylor, I.L., 1998. The origin and mode of fibroblast migration and proliferation in granulation tissue. British Journal of Plastic Surgery 51 (6), 455–461.
Tranquillo, R.T., Murray, J.D., 1992. Continuum model of fibroblast-driven wound contraction: inflammation-mediation. Journal of Theoretical Biology 158, 135.
van der Meulen, M.C.H., Huiskes, R., 2002. Why mechanobiology? Journal of Biomechanics 35 (4), 401–414.
Zohar, R., Cheifetz, S., McCulloch, C.A.G., Sodek, J., 1998. Analysis of intracellular osteopontin as a marker of osteoblastic cell differentiation and mesenchymal cell migration. European Journal of Oral Science 106, 401–407.